Mat. Res. Soc. Symp. Proc. Vol. 677 © 2001 Materials Research Society

Computational model for multiscale simulation of laser ablation

Leonid V. Zhigilei*

Department of Materials Science & Engineering, University of Virginia, Charlottesville, Virginia 22904

ABSTRACT

Multiscale computational approach that combines different methods to study laser ablation phenomenon is presented. The methods include the molecular dynamics (MD) breathing sphere model for simulation of the initial stage of laser ablation, a combined MD - finite element method (FEM) approach for simulation of propagation of the laser-induced pressure waves out from the MD computational cell, and the direct simulation Monte Carlo (DSMC) method for simulation of the ablation plume expansion. The multiscale approach addresses different processes involved in laser ablation with appropriate resolutions and, at the same time, accounts for the interrelations between the processes. A description of the ablation plume appropriate for making a connection between the MD simulation of laser ablation and the DSMC simulation of the ablation plume expansion is discussed.

INTRODUCTION

The interaction of laser pulses with organic matter leading to the massive material removal (ablation) from a target is a subject of scientific as well as applied interest [1,2]. Important practical applications include laser surgery, matrix-assisted laser desorption/ionization (MALDI) of biomolecules for mass - spectrometric investigations, and surface microfabrication of polymer thin films.

During the last several years extensive experimental [1-6], computational [7-16], and theoretical [2,17] efforts have resulted in considerable progress in understanding of many aspects of laser ablation of organic materials. In a big part this progress is due to the development of advanced computational methods and their application to various processes induced by pulsed laser irradiation. In particular, a molecular-level breathing sphere model has yielded a wealth of information on the microscopic mechanisms of laser ablation [7,9,13], parameters of the ejected plume (velocity distributions of matrix and analyte molecules in MALDI [8,10], cluster ejection [11,12,13]) and their dependence on the irradiation conditions (laser fluence [7,9,11], pulse duration [13], initial temperature of the sample [12]). At smaller time- and length-scales, conventional atomic-level MD simulations have demonstrated the ability of this technique to provide detailed information on the dynamics of intermolecular redistribution of the deposited laser energy [14,16] and conformational changes in the molecules undergoing laser desorption [15]. Atomic-level MD simulation technique has been also applied to laser ablation of inorganic materials and first interesting results have been reported [18,19,20]. At the level of the plume expansion, direct simulation Monte Carlo [21-24] and particle-in-cell [25,26,27] methods has been shown to be suitable for realistic simulations of the multi-component ablation plume development on the time- and length-scales of a real experimental configuration. The effects of spatial segregation of light and heavy particles in the plume [23,24], the influence of ionic

* E-mail: lz2n@virginia.edu

species (plasma formation) on the flow process [25,26], and ion extraction by an external field [26] are the examples of the important processes in the ablation plume that can be addressed by these methods.

However impressive the recent advances are, the overall picture of laser ablation still remains rather fragmented. The main obstacle for further progress in understanding of the mechanisms of laser ablation is the lack of connections between the different levels of description of this complex multiscale phenomenon. Each model addresses specific processes with a specific resolution, whereas the real processes occurring at different time- and length-scales are strongly coupled and interrelated.

In this paper, a computational approach that combines different methods (BS, DSMC, FEM) within a single multiscale model is discussed. The multiscale approach addresses different processes involved in laser ablation with appropriate resolutions and, at the same time, accounts for the interrelations between the processes. A general description of the elements of the multiscale model for laser ablation is presented in the next section and is followed by a more detailed discussion of the connection between the MD simulation of the initial stage of laser ablation and DSMC simulation of the ablation plume expansion.

MULTISCALE MODEL FOR LASER ABLATION

The hierarchy of computational methods used to simulate different processes involved in laser ablation with appropriate resolutions is schematically illustrated in Figure 1. Part A represents atomic-level simulations that can be used to study the channels and rates of the vibrational relaxation of molecules excited by photon absorption [14,16,28]. The information on the rates of the conversion of the internal energy of the excited molecules to the translational and internal motion of the other molecules can be verified in pump-probe experiments and can be used for parameterization of the coarser-grained breathing sphere model designed for large-scale MD simulation of laser ablation, Part B of Figure 1. In the breathing sphere model each molecule (or an appropriate group of atoms) is represented by a single particle that has the true translational degrees of freedom but an approximate internal degree of freedom [7]. This internal (breathing) mode allows one to reproduce a realistic rate of the conversion of internal energy of the molecules excited by the laser to the translational motion of the other molecules. Since the molecules rather than the atoms are the particles of interest in the model, the system size can be large enough to model the collective dynamics leading to laser ablation and damage. Moreover, since we are not following high frequency atomic vibrations, we can use a much longer time-step in the numerical integration and keep track of the processes in the simulated system for a longer time [13].

One effect that cannot be directly simulated within the breathing sphere model is the propagation of the laser-induced pressure waves from the absorption region deeper into the bulk of the irradiated sample. The dynamic boundary condition has been developed for computationally efficient simulation of non-reflective propagation of the pressure wave through the boundary of the MD computational cell, allowing to restrict the area of the MD simulation to the region where active processes of laser induced melting, ablation and damage occur [29]. An alternative approach to the problem of pressure wave reflection is to combine the MD model with the continuum finite element method [30], Part C of Figure 1. The advantage of this approach is the ability to study the long-range propagation of the waves and their interaction with other MD regions of a large system. One possible effect of such interaction is schematically

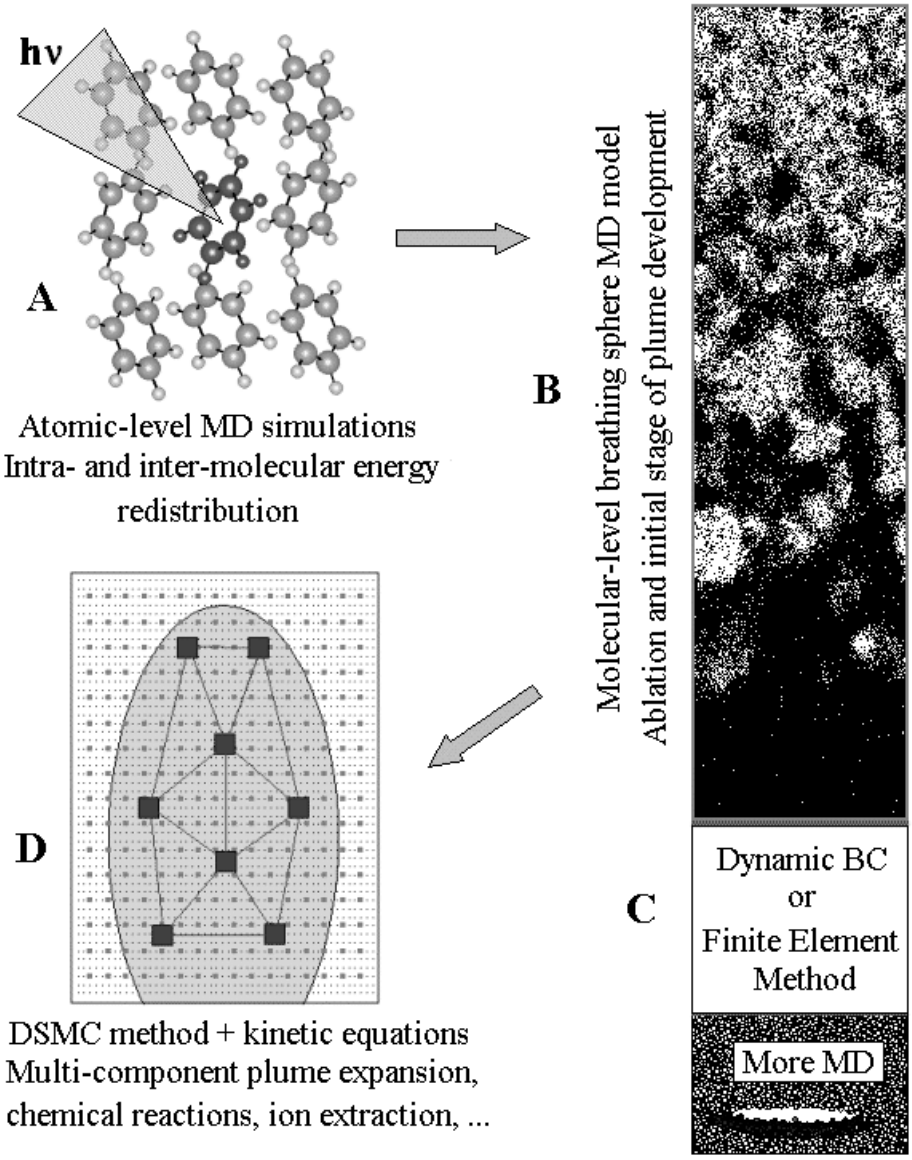

Figure 1. Schematic representation of the hierarchy of computational methods used to simulate processes involved in laser ablation (see explanation in the text).

illustrated in part C of Figure 1. The reflection of the compressive (due to the ablation recoil) pressure wave from the free surface at the back of the irradiated sample can cause the effect known as back spallation [31], when the dynamic tensile strength of the material is exceeded by the reflected (tensile) pressure wave and fracturing occurs at certain depth under the back surface.

The plume development in MD simulation, Part B of Figure 1, can be followed up to a few nanoseconds only, whereas the real time-scales of plume expansion relevant to MALDI and pulsed laser deposition experiments are in the range of microseconds [6]. The long-term plume expansion can be simulated by the DSMC method, Part D in Figure1. The two fine grids in this figure represent the spatial resolution in the DSMC simulation of the plume expansion as well as kinetics of chemical reactions and cluster evaporation. The latter provides input for DSMC

calculations that take into account the change in the relative fractions of plume components. The coarse grid and the squares in Figure 1 represent MD simulations of cluster-cluster and cluster-monomer collisions that are subsequently incorporated into DSMC simulation. The initial conditions for DSMC simulation are provided by the MD breathing sphere model simulations. The description of the ablation plume appropriate for making a connection between the MD simulation of laser ablation and the DSMC simulation of the ablation plume expansion is discussed in the next section.

ANALYSIS OF THE ABLATION PLUME (Connection between the MD and DSMC)

In order to adopt the results of MD simulation of laser ablation as input for DSMC method, we have to describe the MD results on the plume composition and velocities of different plume components in terms usable for DSMC. As an example, below we perform an analysis of the plume for a particular MD simulation of laser ablation of a molecular solid. The simulation is performed for laser pulse duration of 15 ps, fluence of 61 J/m^2, and laser penetration depth of 50 nm. The laser fluence used in this simulation is 2.1 times the threshold fluence for the onset of the massive material ejection or ablation [13]. In order to address the dynamics of the cluster formation during the initial stage of the ablation plume development, in the present study we have to use a significantly larger computational cell as compared to the simulations reported before [7-13,27,29]. The results shown in Figures 2 and 3 are obtained using a computational cell with dimensions of 40×40×90 nm (1 015 072 molecules). The results shown in Figures 4-7 are obtained using a computational cell with dimensions of 40×10×90 nm (253 808 molecules).

The first question that we should address is at what time is it appropriate to switch from MD simulation to DSMC? To answer this question we should study the dynamics of the ablation plume formation and to make sure that the most active processes of the initial plume formation are over before we switch to DSMC. One way to analyze the dynamics of the plume development is schematically illustrated in Figure 2. Computational cell is divided into layers that contain the same number of molecules (10% of the plume = 3 nm of the original solid ≈ 34000 molecules in 40×40×90

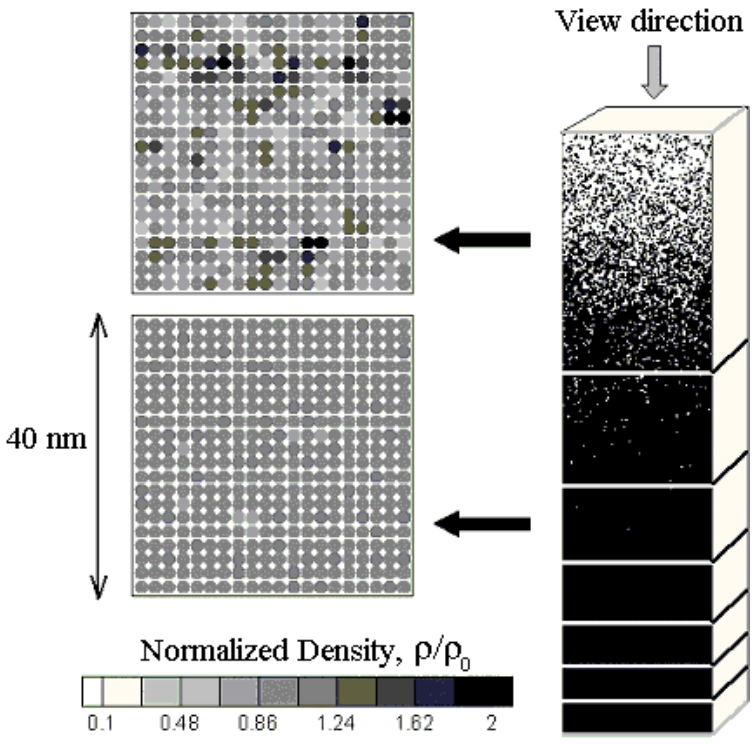

Figure 2. Schematic illustration of the method used to analyze the dynamics of cluster formation in the ablation plume (see Figure 3). Computational cell is divided into layers. Each layer contains the same number of molecules. Density distributions for the same layer are calculated at different times during the simulation.

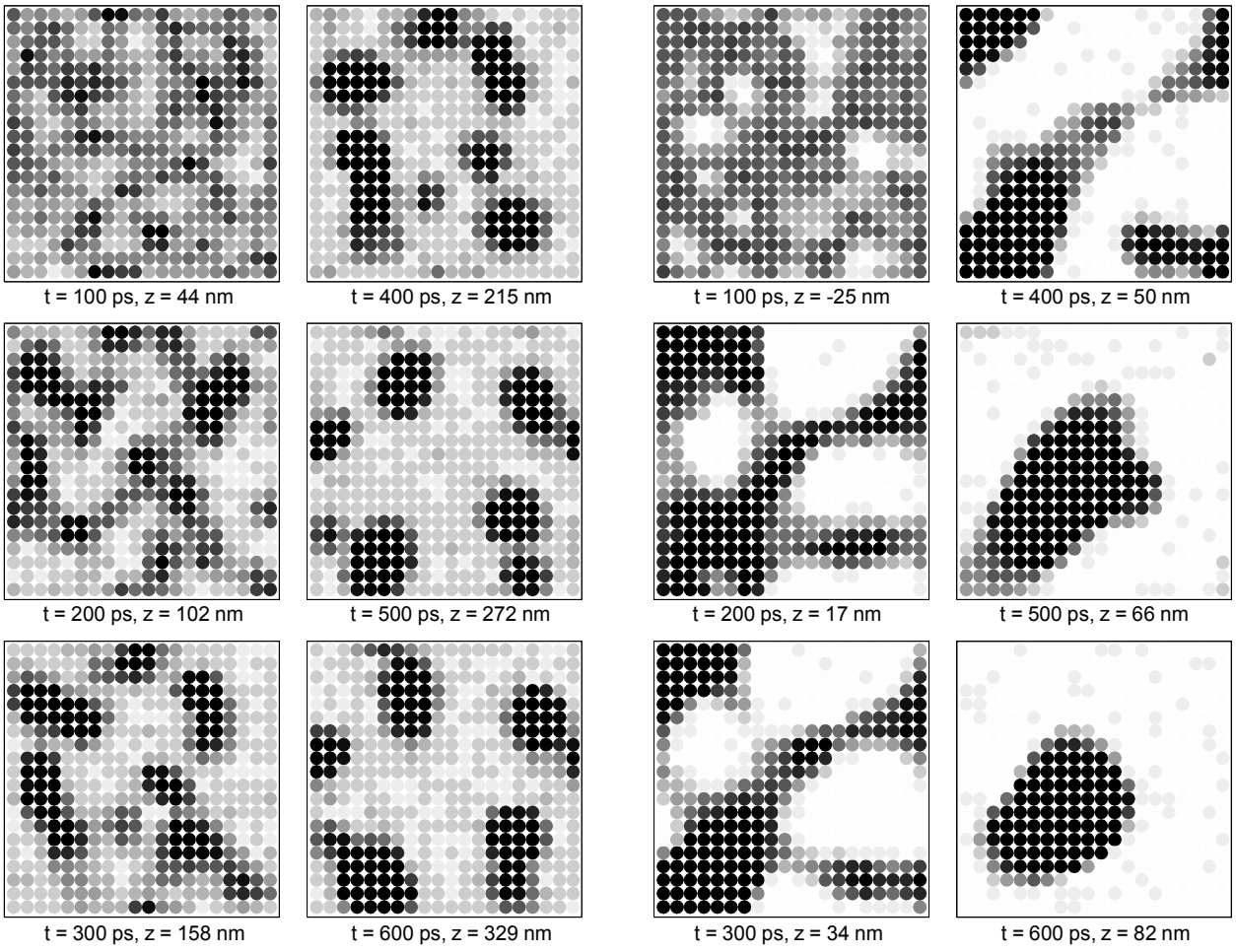

Figure 3. Density plots showing the dynamics of cluster formation in the middle (a) and in the rear part (b) of the ablation plume. Time, t, and layer position relatively to the initial surface of the irradiated target, z, are shown in the figure. Layer position z is the average of the positions of all molecules that belong to the layer. Initial positions at t = 0 are z = -7.5 nm for layer shown in (a) and z = -22.5 nm for layer shown in (b). See Figure 2 for explanation and scale of the contour plots.

nm computational cell) and density distributions for the same layer are calculated at different times. This analysis shows that the dynamics of the cluster formation is different in different parts of the ablation plume and is related to the character of the explosive disintegration of the material [13] that originates from different depths under the surface. The material ejected from the top layers of the irradiated sample is highly overheated and is quickly, within first 100 ps, decomposing into very small clusters and gas phase molecules. The degree of overheating is smaller in the middle of the ejected plume and larger clusters result from the explosive decomposition, Figure 3a. The process of cluster formation in this part of the plume takes up to 400 ps. Formation of the largest clusters, up to 20 nm in diameter, is observed in the rear part of the plume and takes even longer time, Figure 3b. Well-defined large spherical droplets are formed in the rear part of the plume on the timescale of one nanosecond. A further development

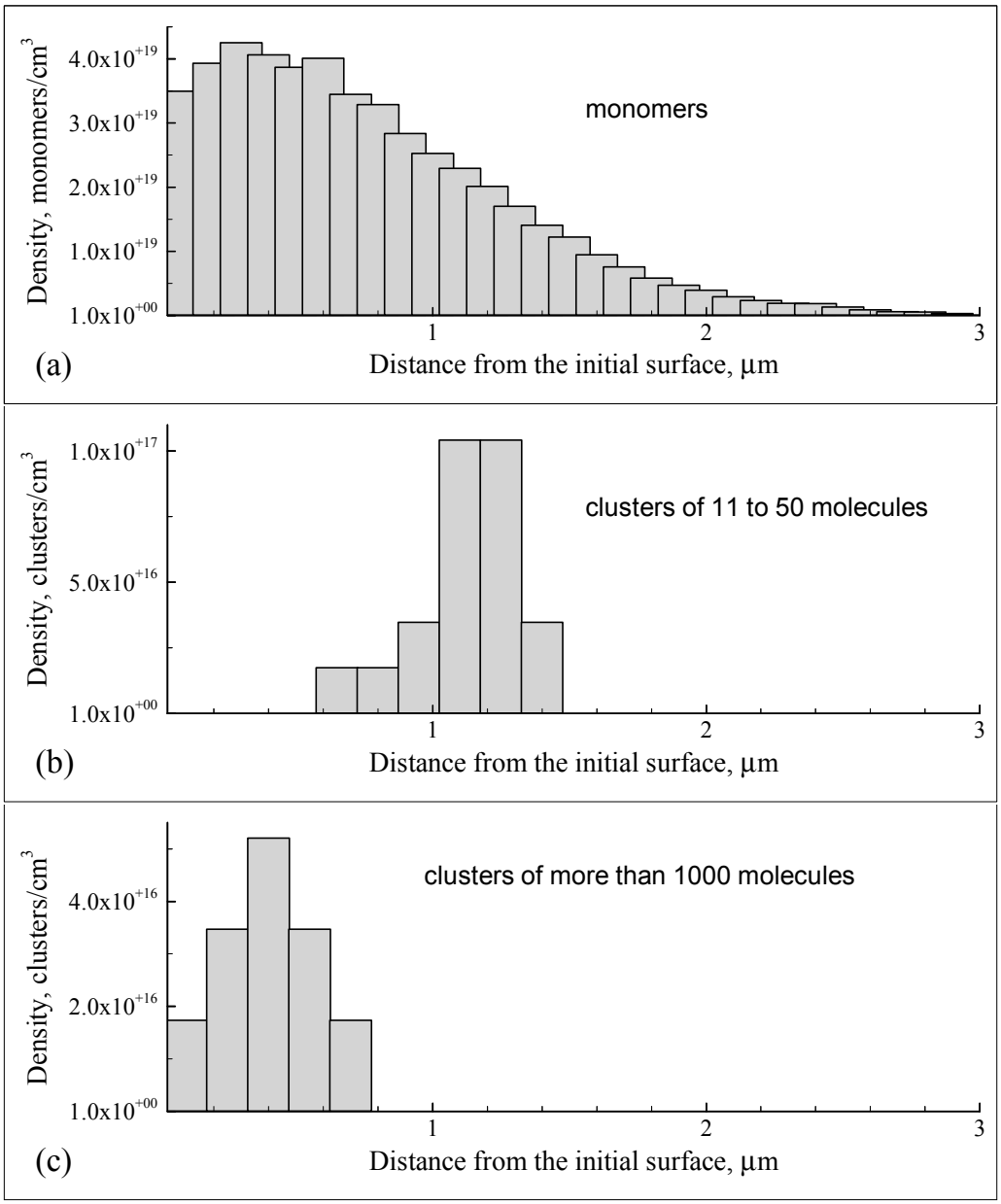

Figure 4. Number density of clusters of different sizes in the ablation plume as a function of the distance from the initial surface. The data is shown for 1 ns after irradiation with 15 ps laser pulse.

of cluster composition of the plume due to the evaporation and cluster-cluster collisions can be incorporated into the DSCM model [32]. Therefore, MD simulation results obtained by the end of 1 ns can be used as input for a DSMC simulation of further plume development.

The next step in making a connection between the MD and DSMC simulations is to describe the parameters of the ejected plume in terms of velocity and cluster size distributions. The clusters observed in MD simulations can be as large as 5000 molecules and the number of clusters of any given size (except for the smallest clusters composed of ~7 or less molecules) is

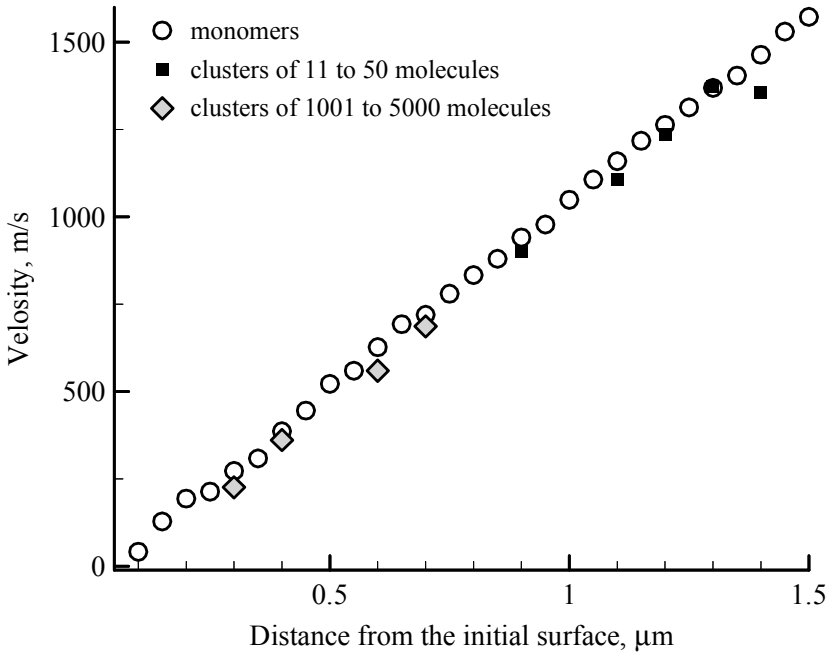

Figure 5. Flow velocity in the direction normal to the irradiated surface for different components of the ablation plume calculated at 1 ns after irradiation with 15 ps laser pulse.

not sufficient to provide a statistically adequate representation of the spatial distribution of clusters in the plume. One possible solution of this problem is to divide clusters into groups. The range of cluster sizes that form a group is chosen so that clusters in a group have similar spatial distribution in the plume. Three example distributions, for individual molecules, for medium-size molecular clusters (11 to 50 molecules), and for large molecular clusters composed of more than 1000 molecules are shown in Figure 4. The distribution in Figure 4b shows that the medium size clusters that result from the plume formation process illustrated by Figure 3a are localized in the middle of the expanding plume, whereas the large clusters formed later during the plume development, Figure 3b, tend to be slower and are closer to the original surface. The relative fractions of clusters within the same size group can be defined by the overall cluster size distribution that is found to follow a power law with power parameter different for low- and high-mass clusters.

In order to describe the velocities of the ejected molecules and clusters we consider the distributions of radial (parallel to the surface) and axial (normal to the surface) velocity components, as well as the flow velocity in the direction normal to the surface for different parts of the plume and for different plume components. The plot of the flow velocity as function of the distance from the initial surface, Figure 5, shows that identical linear dependencies on the distance from the surface, characteristic for the free expansion model, are established for all components of the plume. The clusters of different sizes are entrained into the expanding plume and are moving along with the individual molecules with nearly the same velocities. This effect of entrainment of molecular clusters can be related to the entrainment of large biomolecules into the plume of smaller matrix molecules in MALDI that has been observed experimentally [6] and in MD simulations [7,10].

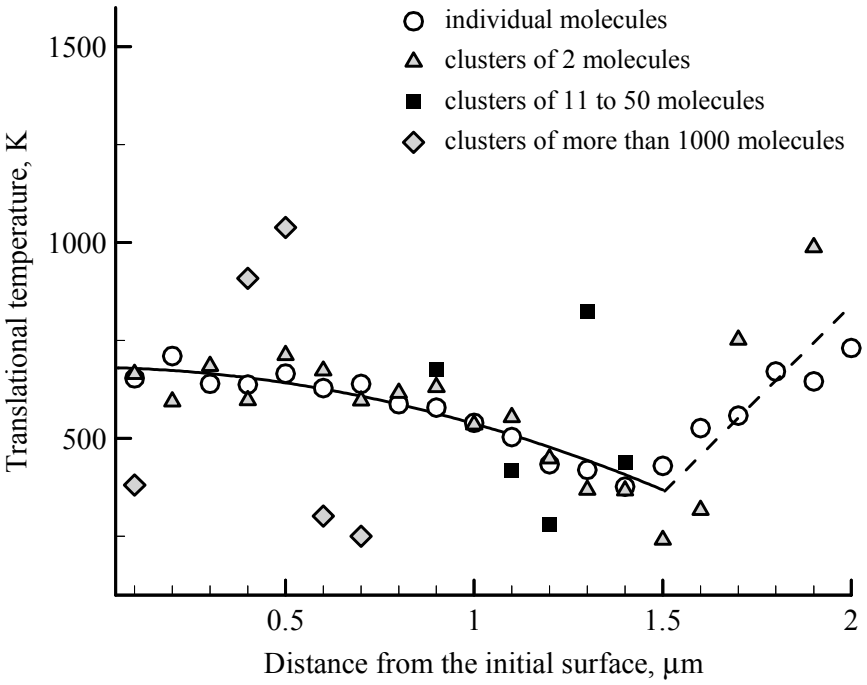

Figure 6. Translational temperature of the plume components as a function of the distance from the initial surface. The translational temperature is calculated from the radial (parallel to the surface) velocity components of the ejected molecules or clusters. The solid and dashed lines show schematically the expansion cooling and the "temperature" increase due to the lack of collisions/equilibration in the front part of the expanding plume, respectively. The data is shown for 1 ns after irradiation with 15 ps laser pulse.

The spread in the radial and axial velocities at a given distance from the surface can be described by a local translational temperature. The radial velocity components of molecules or clusters in the plume does not contain a contribution from the forwarded flow of the plume in the direction normal to the surface and thus can be associated with the thermal motion in the plume. As found in earlier simulations [8,10,13], the radial velocity distributions of ejected molecules fit well to a Maxwell-Boltzmann distribution substantiating the association of the spread of the radial velocities with the thermal motion. Thus, the local translational temperatures of the plume components are calculated from the radial (parallel to the surface) velocity components of the ejected molecules or clusters.

A spatially resolved analysis of the translational temperature of the plume reveals a significant temperature variation with distance from the irradiated surface, Figure 6, suggesting that the fast cooling of the ejected material proceeds nonuniformly within the plume. Expansion cooling, when the thermal energy is transformed to the kinetic energy of the plume expansion, leads to the decrease of the temperature in the flow direction. A large scattering of the data points observed in Figure 6 for large clusters is due to the small number of clusters in these groups. Although the poor statistics does not allow us to perform a reliable estimation of the translational temperature for the large clusters, simulation results suggest that the same local translational temperature can be used to describe the spread of the radial velocities of different plume components in the dense part of the plume. A series of simulations for the same laser

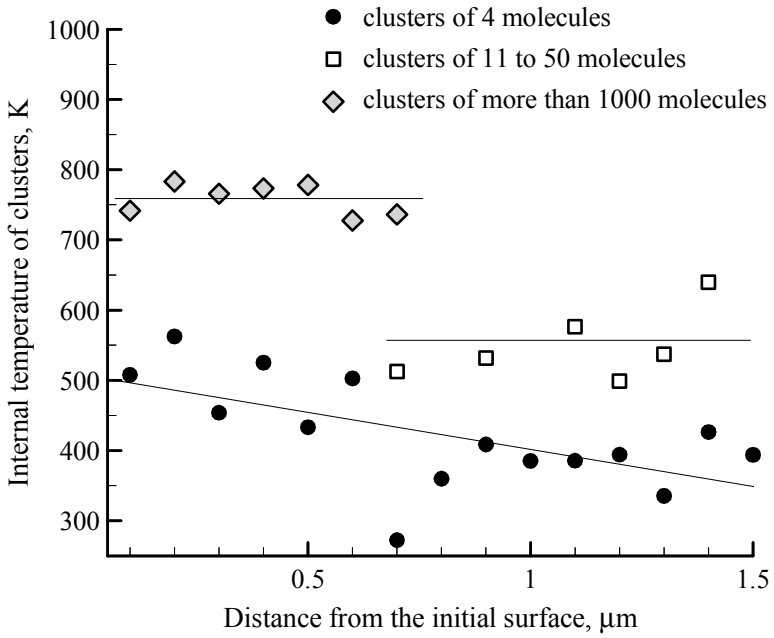

Figure 7. Internal temperature of the ejected clusters as a function of the distance from the initial surface. The internal temperature is calculated from the kinetic energy of the molecular motion in the center of mass frame of reference. Lines are just guides to the eye. The data is shown for 1 ns after irradiation with 15 ps laser pulse.

fluence is being performed in order to obtain statistically significant data and verify this hypothesis. The effect of the local thermal equilibration of different plume components can be related to the earlier results of MD simulations of MALDI, when the radial velocity distributions for both matrix molecules and analyte molecules of different masses were found to fit well to a Maxwell-Boltzmann distribution with the same temperature [10]. At certain distance from the surface, the translational temperature of monomers and small clusters reaches its minimum and starts to increase. This temperature increase can be attributed to the lack of equilibration in the front part of the expanding plume, where too small densities of ejected molecules are observed.

Finally, the knowledge of the internal temperature of clusters in the ablation plume is needed for realistic representation of cluster-cluster collision events and cluster evaporation/growth processes in DSMC simulations of the long-term plume development. The internal temperature of a cluster is defined from the kinetic energy of the molecular motion in the center of mass frame of reference and shown for three groups of clusters in Figure 7. Large clusters in the plume are found to have substantially higher internal temperatures as compared to the smaller clusters and to the translational temperature of the surrounding gas phase molecules, reflecting a slower cooling by evaporation as compared to the fast expansional cooling. The description of the ablation plume, shortly described above, provides a realistic input for DSMC simulations of the further development of the multi-component ablation plume on the time- and length-scales of real experimental configurations [32].

SUMMARY

A computational approach that combines different methods within a single multiscale model is demonstrated to be capable of addressing different processes involved in laser ablation with appropriate resolutions and, at the same time, accounts for the interrelations between the processes. The multiscale approach includes the molecular dynamics breathing sphere model for simulation of the initial stage of laser ablation, a combined molecular dynamics - finite element method for simulation of propagation of the laser-induced pressure waves out from the MD computational cell, and the direct simulation Monte Carlo method for simulation of the ablation plume expansion. A description of the ablation plume appropriate for making a connection between the MD simulation of laser ablation and the DSMC simulation of the ablation plume expansion is presented.

ACKNOWLEDGMENTS

The author would like to thank Barbara J. Garrison, Alexei G. Zhidkov, and Michael Zeifman for insightful and stimulating discussions and suggestions.

REFERENCES

1. *Proceedings of the 5th International Conference on Laser Ablation*, edited by J. S. Horwitz, H.-U. Krebs, K. Murakami, M. Stuke, Appl. Phys. A **69** [Suppl.] (1999).
2. D. Bäuerle, *Laser Processing and Chemistry* (Springer-Verlag, Berlin Heidelberg, 2000).
3. K. Dreisewerd, M. Schürenberg, M. Karas, and F. Hillenkamp, Int. J. Mass Spectrom. Ion Processes **141**, 127 (1995).
4. M. Karas, M. Glückmann, and J. Schäfer, J. Mass Spectrom. **35**, 1 (2000).
5. M. Handschuh, S. Nettesheim, and R. Zenobi, Appl. Surf. Sci. **137**, 125 (1999).
6. A. A. Puretzky, D. B. Geohegan, G. B. Hurst, M. V. Buchanan, and B. S. Luk'yanchuk, Phys. Rev. Lett. **83**, 444 (1999).
7. L. V. Zhigilei, P. B. S. Kodali, and B. J. Garrison, J. Phys. Chem. B **101**, 2028 (1997); ibid., **102**, 2845 (1998).
8. L. V. Zhigilei and B. J. Garrison, Appl. Phys. Lett. **71**, 551 (1997).
9. L. V. Zhigilei, P. B. S. Kodali, and B. J. Garrison, Chem. Phys. Lett. **276**, 269 (1997).
10. L. V. Zhigilei and B. J. Garrison, Rapid Commun. Mass Spectrom. **12**, 1273 (1998).
11. L. V. Zhigilei and B. J. Garrison, Appl. Phys. Lett. **74**, 1341 (1999).
12. L. V. Zhigilei and B. J. Garrison, Appl. Phys. A **69**, S75 (1999).
13. L. V. Zhigilei and B. J. Garrison, J. Appl. Phys. **88**, 1281 (2000).
14. X. Wu, M. Sadeghi and A. Vertes, J. Phys. Chem. B **102**, 4770 (1998).
15. M. Sadeghi, X. Wu, and A. Vertes, J. Phys. Chem. B **105**, 2578 (2001).
16. Ł. Dutkiewicz, R. E. Johnson, A. Vertes, and R. Pędrys, J. Phys. Chem. A **103**, 2925 (1999).
17. R. E. Johnson, -in *Large Ions: Their Vaporization, Detection and Structural Analysis*, edited by T. Baer, C. Y. Ng, I. Powis (John Wiley: New York, 1996) p. 49.

18. E. Ohmura and I. Fukumoto, Int. J. Japan Soc. Prec. Eng. **30**, 128 (1996).
19. R. F. W. Herrmann, J. Gerlach, and E. E. B. Campbell, Appl. Phys. A **66**, 35 (1998).
20. P. Lorazo, L. J. Lewis, and M. Meunier, Appl. Surf. Sci. **168**, 276 (2000).
21. G. A. Bird, *Molecular gas dynamics and the direct simulation of gas flows* (Clarendon Press, Oxford, 1994).
22. D. Sibold and H. M. Urbassek, J. Appl. Phys. **73**, 8544 (1993).
23. H. M. Urbassek and D. Sibold, Phys. Rev. Lett. **70**, 1886 (1993).
24. T. E. Itina, J. Appl. Phys. **89**, 740 (2001).
25. C. K. Birdsall, IEEE Trans. Plasma Sci. **19**, 65 (1991).
26. A. G. Zhidkov, Phys. Plasmas **5**, 541 (1998).
27. A. G. Zhidkov, L. V. Zhigilei, A. Sasaki, and T. Tajima, Appl. Phys. A, in press.
28. T.-C. Chang, D. Dlott, J. Chem. Phys. **90**, 3590 (1989).
29. L. V. Zhigilei and B. J. Garrison, in *Multiscale Modelling of Materials*, Mater. Res. Soc. Proc. **538,** 491 **(**1999).
30. J. A. Smirnova, L. V. Zhigilei, and B. J. Garrison, Comput. Phys. Commun., **118**, 11 (1999).
31. E. Dekel, S. Eliezer, Z. Henis, E. Moshe, A. Ludmirsky, and I. B. Goldberg, J. Appl. Phys. **84**, 4851 (1998).
32. M. Zeifman, L. V. Zhigilei, and B. J. Garrison, in preparation.